

# RADIATION DAMAGE IN HST DETECTORS

Marco Sirianni, *European Space Agency, Space Telescope Science Institute*

Max Mutchler, *Space Telescope Science Institute*

Abstract: We present an analysis of the radiation damage in CCDs on board of the Hubble Space Telescope. We describe the radiative environment of the HST and the impact seen in the ACS, WFPC2 and STIS CCDs in terms of dark current, hot pixels and charge transfer efficiency.

Key words: HST, Radiation Damage, CTE, Hot Pixels, Annealing

## 1. INTRODUCTION

The Hubble Space Telescope (HST) has been orbiting in a low earth orbit (LEO) since April 1990. A large variety of scientific instruments have been installed on HST, each with a unique set of detectors (Table 1).

*Table 1.* Detector type and years on orbits for the main instruments of HST.

Detector type	Instrument	# of chips	Year on orbit
CCD	WFPC	8	3.5 (1990-1993)
	WFPC2	4	> 12 (1993- present)

Detector type	Instrument	# of chips	Year on orbit
	STIS	1	> 8 (1997-2004)
	ACS	3	> 3 (2002- present)
	WFC3	2	0 (TBD)
	Tot	16 (+2)	
IR	NICMOS	3	> 8 (1997- present)
	WFC3	1	0 (TBD)
	Tot	3 (+1)	
UV-MCP	SITS	2	> 8 (1997-2004)
	ACS	1	> 3 (2002- present)
	COS	1	0 (TBD)
	Tot	3 (+1)	

## 2. HST RADIATION ENVIRONMENT

HST orbits in a Low Earth Orbit, at about 580 km of altitude with an inclination of 28 degrees. Every day HST completes about 15 orbits and on average HST orbit crosses some portion of the South Atlantic Anomaly (SAA) region seven times/day.

The SAA is the region where the Earth's inner radiation belt makes its closest approach to the planet's surface. The inner belt contains mostly protons with energy between 10 and 50 Mev but also electrons, lower energy protons, cosmic ray ions. The population of trapped particles with the belts is not static. Increase in solar activity expands the atmospheres and increases the losses of protons in LEO. Therefore, trapped radiation doses in LEO decrease during solar maximum and increase during solar minimum.

When HST transits a portion of the SAA, all its detectors are exposed to several minutes of strong radiation. Although the radiation environment is the same for all of them, the unique properties of these devices pose different challenges to their functionality in space.

For this paper we will focus on the radiation impact seen in CCDs on board of HST. The amount of data available for this analysis varies among the instruments, with younger instruments being better monitored than older ones. We therefore restrict this talk to the ACS, STIS and WFPC2 devices (see Table 2).

Two very good reviews have been published in recent years. Pickel et al. (2003) and Srour et al. (2003) provide a summery of the evolution of radiation effect understanding in infrared detector technology, CCDs and active pixels sensors.

Radiation damage mechanisms in CCDs are divided into two general categories: total ionizing dose (TID) and displacement damage effects (see Srour et al 2003 and Clampin et al 2005). Since all the HST detectors are a buried channel and are operated inverted they are mainly subject to displacement damage and almost completely insensitive to charge generation and accumulation at the silicon-oxide interface, which is typical of TID damage. Displacement damage refers to the introduction of defects in the silicon lattice. Charged particles such as protons and neutrons can collide with silicon atoms and displace them from their lattice sites. This process results in vacancy-interstitial pairs, most of which immediately recombines. The vacancies that survive migrate in the lattice and form stable defects. Any defect gives rise to a new energetic level in the bandgap and therefore alter the electrical and optical performance of the device.

These defects degrade CCD performance by decreasing the charge transfer efficiency (CTE), increasing the mean dark current and dark current non-uniformity by introducing individual pixels with very high dark current (also known as hot pixels or hot spikes).

Table 2. Basic HST/CCD specifications

	ACS/WFC	ACS/HRC	STIS	WFPC2
	SITe	SITe	SITe	Loral
Qt. -Size (pixel)	2- 4096x2048	1- 1024x1024	1 – 1024x1024	4- 800x800
Pixel size ( $\mu\text{m}$ )	15	21	21	15
Architecture	3-phase thin- back ill.	3-phase thin- back ill.	3-phase thin - back ill.	3-phase thick –front ill.
Temperature (C)	-77	-81	-83	-88
Readout	2 amp / MPP	1 amp /MPP	1 amp/MPP	1 amp /MPP
Parallel clock (Hz)	20	40	42	60
Minichannel	3 $\mu\text{m}$	3 $\mu\text{m}$	3 $\mu\text{m}$	-

### 3. ANALYSIS OF THE RADIATION DAMAGE

#### 3.1 Dark Rate

In the depletion region of each pixel, energy levels near midgap are responsible for generation of electron-hole pairs. Thermal excitation of a bound valence-band electron to the defect energy level can be followed by another excitation to the conduction band, thus generating a free electron-hole pair. Multi Phinned Phase (MPP) devices are run into inversion and

therefore the surface dark current is suppressed and the bulk dark current is the only contribution.

The average dark current increase correlates with the amount of displacement damage imparted by incoming protons. This behavior is seen on all HST CCDs as shown in Table 3. It is interesting to note that after approximately five years after installation, the dark current for WFPC2 CCDs stopped increasing linearly. The reason for this behavior is still under investigation. It is known (Biretta et al. 2001) that the dark rate in WFPC2 is produced by two components. The first one is the classical thermal generation of electron-hole pairs at the pixel level, the second one is related to the fluorescence of the MgF<sub>2</sub> window, which correlate with the solar cycle.

Table 3. Dark Rate Increase as a function of time for HST CCDs

	WFC	HRC	STIS	WFPC2
e-/pix/hr/year	1.5 WFC1 2.0 WFC2	2.1	3.3 (side 1) 2.2 (side 2)	2.0 (1993- 1998) ~ 0 (> 1998)
Temperature (C)	-77	-81	-83 (side 1) < -83 (side 2)	-88

### 3.2 Hot Pixels and Annealing

Although the increase in the mean dark rate with proton irradiation is important the dark current non-uniformity (hot pixels) is generally a bigger concern for astronomical applications. Some pixels show very high dark current up to several times the mean dark rate. Depending on the particular collision sequence, protons of the same energy may produce very different amount of displacement damage. Moreover, if a defect is created in a high electric field region, the contaminated pixel can show very large dark current as a result of field-enhanced emissions (Dale et al. 1990).

Hot pixels accumulate as a function of time on orbit. Figure 1 shows the evolution with time of the distribution of pixels at different dark rate for one of ACS/WFC CCDs. As the proton-induced damage increases the mean dark current (the peak of the distribution) and the hot pixels population (the tail of the histogram) increase. According to Hopkinson et al (1996) a simple fit to the histogram can be made assuming a Gaussian main peak whose half-width increases approximately as the square root of the fluence, and an exponential tail whose amplitude is proportional to fluence.

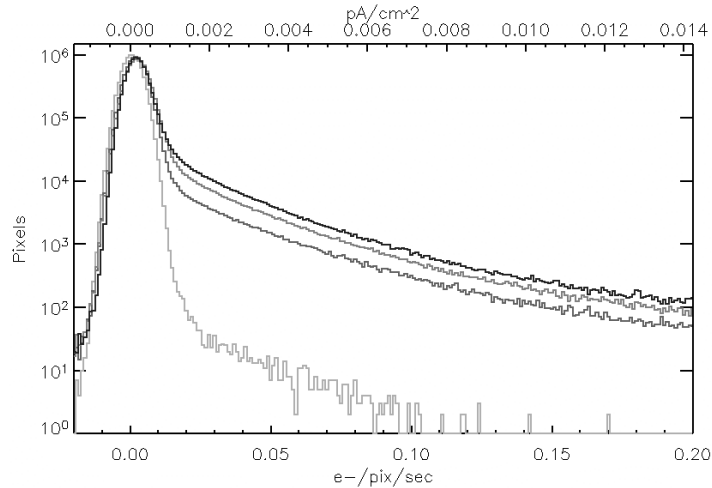


Figure 1. Distribution of dark pixels for one WFC CCD at launch (2002) (at bottom), and after 1,2 and 3 years on orbit.

Sirianni et al (2004) discussed the evolution of hot pixels in the ACS CCDs and find that the number of new hot pixels with a dark current higher than the mean dark current increases every day by few to several hundreds depending on the threshold used (see Table 4). In order to partially anneal the hot pixels, all HST instruments perform monthly anneal, by raising the CCD temperature to about +20 C for few hours. Although it is still not clear why at such low temperature a significant annealing is observed (the most common defects in silicon anneal at much higher temperature), we can report a few interesting findings (see Sirianni et al. 2005 for more details):

- The annealing rate strongly depends on the dark rate of the hot pixel. Very hot pixels show a higher anneal rate than warmer pixels and there is no impact on the average dark current level (Sirianni et al. 2004).
- The same anneal rate can be obtained at colder temperatures. In at least four instances, in occurrence of HST safing events, the temperature of ACS CCDs raises to -10C for periods ranging between 24 and 48 hours. After these periods the population of hot pixels decreased by the same amount as in a normal anneal cycle at +20 C.
- The anneal rate does not seem to be related to the length of the anneal. Since launch the anneal time for ACS CCDs have been reduced first from 24 to 12 hrs and more recently from 12 to 6 hr without impacting the annealing effectiveness.
- For any particular hot pixel, a complete anneal is a rare event. Most of the annealed hot pixels significantly reduce their dark current level but never rejoin the population of normal (Gaussian distribution) dark pixels.

- Several hot pixels show evidence of reverse annealing. While most of the hot pixels show some degree of healing in response to an annealing procedure, some of them may be activated to “hot” by the same procedure. This happens to pixels that have been damaged by radiation and that, depending on the anneal cycle they may lose or regain the status of “hot pixel”. Figures 2 and 3 show examples of normal and reverse annealing respectively.

Table 4. Anneal rate for different HST CCDs

	ACS/WFC		ACS/HRC		STIS		WFPC2	
Temp	-77	C	-81	C	-83	C	-88	C
Annealing Temp	-10 to + 20		-10 to + 20		+5		+30	
Annealing Duration	6 to 24 hr		6 to 24 hr		24 hr		24 hr	
Threshold	%	+/-	%	+/-	%	+/-	%	+/-
> 0.02	0.55	0.02	0.64	0.02			0.80	0.05
> 0.04	0.70	0.07	0.84	0.07				
> 0.06	0.78	0.04	0.84	0.04				
> 0.08	0.82	0.03	0.87	0.03				
> 0.10	0.84	0.02	0.85	0.02	0.77	0.05		
> 1.0	0.55	0.15	0.64	0.15				

### 3.3 Charge Transfer Efficiency

Without any doubt CTE degradation is the radiation damage with the largest impact on the scientific application of CCD in space. The trapping of charge during the readout causes errors in stellar photometry, stellar astrometry and the observed surface brightness of extended objects. There are many techniques to measure the CTE of a CCD. In HST only the flight software of ACS allows to perform Extended Pixel Edge Response (EPER) and First Pixel Response (FPR) tests on orbit. ACS CTE is monitored monthly at the Fe<sup>55</sup> signal level and twice a year over a wide range of signal levels (see Sirianni et al. 2004 and Mutchler et al 2005 for more details). At each signal level the CTE is degrading linearly with time. For ACS and all the other HST CCD –based instruments a corrective formula to apply to photometric measurements to remove the impact of CTE degradation has been derived by observing a star cluster (see for example Riess et al., 2004). By positioning the same star in different positions across the CCD it is possible to measure the amount of charge lost due to CTE problem. By using several stars with different brightness and different filters to simulate different background conditions it is possible to derive a formula that takes into account the signal in the PSF, the position in the chip, the background level and the time of the observation. These tests measure the “missing

charge” and therefore can provide an absolute measurement of CTE. If  $\Delta\text{mag}$  is the missing flux (in magnitude) after the star has been transferred through  $n$  rows the classical CTE figure is:  $\text{CTE} = 10^{(\Delta\text{mag}/2.5n)}$ .

We compared the CTE degradation trend for all HST CCDs in figure 4. For ACS/WFC the results from the EPER test and the photometric test are in perfect agreement. A corrective formula for ACS/HRC is still not available, so we show only the EPER results. The STIS and WFPC2 trends are derived from photometric tests. It is clear that the WFC CCD is degrading much less rapidly than WFPC2 CCDs. A fair comparison should take into account the operating temperature and the clocking rate, which are fundamental factors for CTE performance.

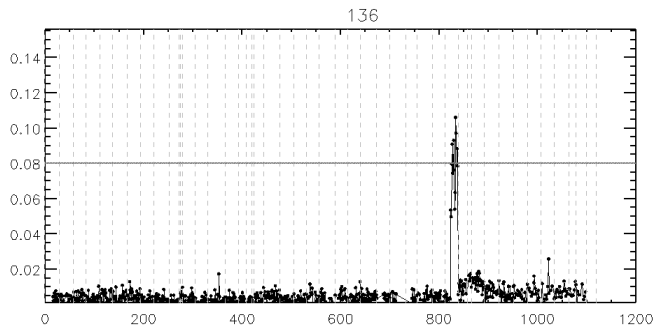


*Figure 2.* Signal level of hot pixel # 136 as a function of time (days). Vertical dashed lines mark the annealing dates. The horizontal line marks the threshold for hot pixel definition. The signal level is in e-/pix/sec at -77 C. The pixel is damaged just after day 800 and it is fully healed after the first annealing cycle.

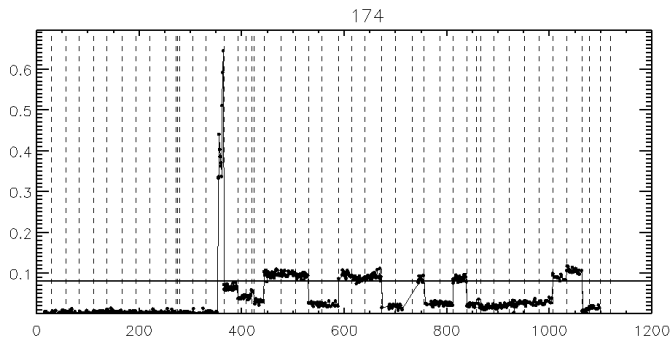


*Figure 3.* Signal level of hot pixel # 174 as a function of time (days). The pixel is damaged after day 350. Following anneal cycles partially heal the pixel whose dark current jumps between discrete levels in correspondence of anneal cycles.

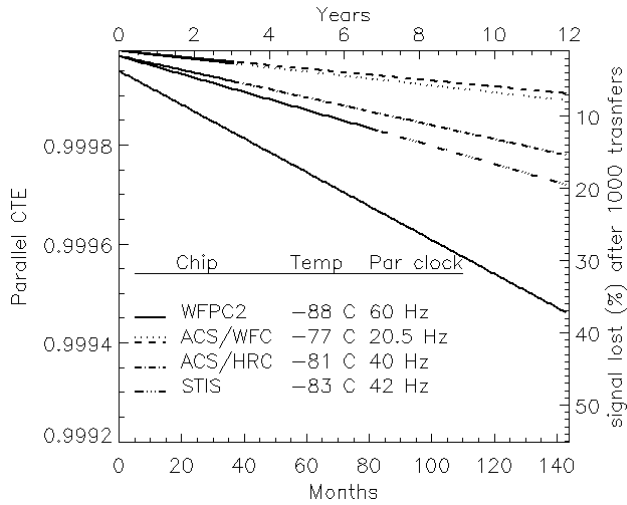


Figure 4. Evolution of parallel CTE as a function of time on orbit. Two lines are shown for ACS/WFC: the dotted line is the trend inferred from the star photometry test, the dashed line is from the EPER test. The solid segment of each line shows the actual time spent on-orbit.

#### 4. REFERENCE

- Dale, C.J., Marshall, P.W, and Burke, E.A. 1990,, IEEE Trans. Nucl. Sci. vol 37, 1784.
- Hopkinson, G.R., Dale, C.J., and Marshall, P.W. 1996, IEEE Trans. Nucl. Sci. vol 43, 614
- Mutchler, M. and Sirianni, M. 2005, ACS –ISR 05-03, STScI (Baltimore, MD)
- Pickel, J.C., Kalma, A.H., Hopkinson, G.R., and Marshall, C.J. 2003, IEEE Trans. Nucl. Sci. vol 50, 671.
- Riess, A., and Mack, J. 2004, ACS –ISR 04-06, STScI (Baltimore, MD)
- Sirianni, M. Mutchler, M., Clampin, M., Ford, H., Illingworth, G., Hartig, G., van Orsow, D., and Wheeler, T. 2004, SPIE Vol 5499, 173.
- Sirianni M. et al.. 2005, “The dark rate and hot pixels in ACS CCDs’ ACS-ISR, STScI (Baltimore, MD) , *in preparation*
- Srouf, J.R., Marshall, C.J., and Marshall, P.W. 2003, IEEE Trans. Nucl. Sci. vol 50, 653.